

Article

## Plasma Treated Multi-Walled Carbon Nanotubes (MWCNTs) for Epoxy Nanocomposites

Andrew C. Ritts<sup>1</sup>, Qingsong Yu<sup>1,\*</sup>, Hao Li<sup>1</sup>, Stephen J. Lombardo<sup>1</sup>, Xu Han<sup>1</sup>, Zhenhai Xia<sup>2</sup> and Jie Lian<sup>3</sup>

<sup>1</sup> Mechanical and Aerospace Engineering Department, University of Missouri, Lafferre Hall, Columbia, MO 65211, USA; E-Mails: rittsa@missouri.edu (A.C.R.); liha@missouri.edu (H.L.); LombardoS@missouri.edu (S.J.L.); hanx@missouri.edu (X.H.)

<sup>2</sup> Department of Material Science and Engineering, University of North Texas, Discovery Park E159A, Denton, TX 76203, USA; E-Mail: Zhenhai.Xia@unt.edu (Z.X.)

<sup>3</sup> Department of Mechanical, Aerospace & Nuclear Engineering, Rensselaer Polytechnic Institute, 110 8th street, Troy, NY 12180, USA; E-Mail: lianj@rpi.edu (J.L.)

\* Author to whom correspondence should be addressed; E-Mail: yuq@missouri.edu; Fax: +1-573-884-5090.

Received: 26 October 2011; in revised form: 8 December 2011 / Accepted: 16 December 2011 / Published: 19 December 2011

---

**Abstract:** Plasma nanocoating of allylamine were deposited on the surfaces of multi-walled carbon nanotubes (MWCNTs) to provide desirable functionalities and thus to tailor the surface characteristics of MWCNTs for improved dispersion and interfacial adhesion in epoxy matrices. Plasma nanocoated MWCNTs were characterized using scanning electron microscopy (SEM), high-resolution transmission electron microscopy (HR-TEM), surface contact angle, and pH change measurements. Mechanical testing results showed that epoxy reinforced with 1.0 wt % plasma coated MWCNTs increased the tensile strength by 54% as compared with the pure epoxy control, while epoxy reinforced with untreated MWCNTs have lower tensile strength than the pure epoxy control. Optical and electron microscopic images show enhanced dispersion of plasma coated MWCNTs in epoxy compared to untreated MWCNTs. Plasma nanocoatings from allylamine on MWCNTs could significantly enhance their dispersion and interfacial adhesion in epoxy matrices. Simulation results based on the shear-lag model derived from micromechanics

also confirmed that plasma nanocoating on MWCNTs significantly improved the epoxy/fillers interface bonding and as a result the increased composite strength.

**Keywords:** polymers; nanocomposites; plasma treatment; dispersion; interfacial adhesion; multi-walled-carbon-nanotubes

---

## 1. Introduction

Polymeric nanocomposites have been an area of intense industrial and academic interests due to their lightweight and significantly improved properties. There is increased research interest in reinforcing polymers with one dimensional nanomaterials with high aspect ratios due to their outstanding mechanical, thermal, and electrical properties [1-4]. One dimensional nanomaterials are preferred as reinforcing materials compared to zero dimensional nanoparticles because nanofibers/nanotubes provide larger load transfer and help facilitate well-known toughening mechanisms, such as fiber bridging, and fiber pullout [5].

Nanocomposite materials are significantly different from conventional micron scale composites in many ways. The high surface area inherent to nanomaterials and comparable size to the gyration radius of polymer chains makes nanomaterials prone to form aggregates in composites and gives a relatively low loading rate (mass fraction) of nanomaterials. Percolation threshold is typically used to describe the maximum of loading rate of reinforcing materials, beyond which adding more reinforcing materials becomes detrimental to the composite properties. The typical percolation threshold for single walled carbon nanotubes in polymers is typically around 0.1–2 vol % [6]. Currently there exist two major challenges in developing novel polymer nanocomposites. First, a homogeneous dispersion of nanofillers in their host polymer matrices is required. Second, an enhanced interfacial adhesion of the nanofillers to the polymer matrix is required to provide effective load transfer from polymer matrix to the nanofillers. If these two major challenging problems are not solved, the nanocomposites fabricated may significantly under-perform their theoretical possibilities.

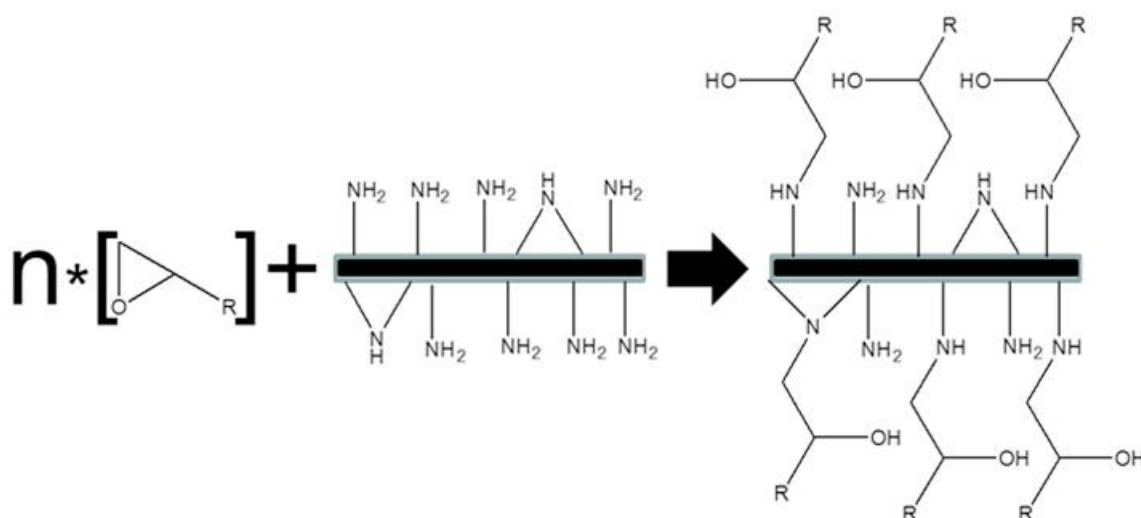
Presently there are several methods for uniformly dispersing nanofillers into the composite resin. These include: melt blending, solvent mixing, and *in situ* polymerization [7]. Both melt blending and *in situ* polymerization are generally superior to solvent mixing in material properties due to difficulty of removing solvents from the composite, which induces voids within the composite, and generally provides a non-uniform filler loading throughout the composite. Melt blending requires heat and large shear forces to break filler agglomerations. It can be energy intensive and can negatively affect the polymers by decreasing the molecular weight and inducing defects in the nanofiller material. *In situ* polymerization requires little capital to fabricate nanocomposites, but adequate dispersion and interfacial adhesion of nanofillers in polymer matrices is still difficult to achieve.

Nanomaterials exhibit novel properties in general; however these novel properties are associated with isolated particles [8]. As an example, in order to take advantage of high strength of carbon nanotubes, it is critical to achieve better dispersion and sufficient CNT-polymer interfacial bonding. A variety of methods have been proposed to avoid agglomeration, including chemical treatments, controlled oxidation, etching, polymer wrapping/absorption, adsorption of amines. Plasma

nanocoatings/modifications have been used to reduce agglomerations by modifying the surface of nanomaterials [9]. Plasma nanocoating of individual nanoparticles in particular proves effective in breaking up nanoparticle agglomeration [10-17]. Plasma nanocoatings generally contain functional groups which electrostatically prevent agglomeration and can also enhance interactions with the polymer matrix. Various plasma methods have been used for surface modification and surface activation/grafting of carbon nanotubes (CNTs). These methods range from low pressure plasmas to atmospheric plasmas, such as corona discharge to dielectric barrier discharge, *etc.* [18-22]. Utilizing plasma methods to treat or modify nanomaterials can widen the range of polymer matrix possibilities, and studying/tailoring those coatings/modifications can increase the nanofillers's dispersion in polymer matrices and enhance the filler/matrix interfacial bonding in order to achieve the desired properties of the resulted polymer nanocomposites.

The objective of this study was to determine the feasibility of utilizing allylamine plasmas to treat and modify MWCNTs for the reinforcement of an epoxy matrix. Allylamine plasma treatment of MWCNTs is hypothesized to increase the dispersion and interfacial adhesion of the MWCNTs through the formation of covalent bonds with epoxide groups in epoxy as schematically illustrated in Figure 1.

**Figure 1.** Schematic illustration of the interfacial reaction between epoxy and allylamine plasma coated MWCNTs after mixing.



## 2. Experimental

MWCNTs of 95% purity were purchased from Helix Material Solutions (Houston, TX, USA) in two sizes (10–30 nm and 60–100 nm diameters) with length ranging from 0.5 to 40  $\mu\text{m}$ . The MWCNTs were characterized by Hitachi S-4700 Scanning Electron Microscope (Schaumburg, IL, USA) and JEOL 1400 Transmission Electron Microscope (Peabody, MA, USA).

Before modifying the surfaces of MWCNTs using plasma nanocoating and thus tailoring their interface with a polymer matrix, a thorough characterization of the filler and matrix material should help determine the treatment type for the filler. Epon 815c resin contains 86.4% bisphenol-A-(epichlorhydrin) and 13.6% N-butyl glycidyl ether, both of which contain at least one epoxide group.

Epicure 3223 curing agent mainly consists of diethylenetriamine, which allows the matrix to crosslink. Surface modification of MWCNTs with plasma nanocoating that contains rich amine groups can allow the filler to be chemically incorporated into the matrix through ring opening reactions of epoxides and thus form covalently interface bonding between the filler and epoxy matrix as schematically illustrated in Figure 1. In this study, allylamine was specifically chosen as the precursors or monomers to deposit plasma nanocoatings for introducing primary amines on plasma coating surfaces while the olefinic double bond promotes the formation of a plasma coating. Mixture of allylamine vapor and argon gas was used as plasma fuel for plasma nanocoating deposition and surface modification of MWCNTs. Addition of argon gas into the plasma system enable us to adjust the deposition rate of plasma nanocoating and thus well control the plasma treatment uniformity of MWCNTs.

Various types of plasma reactors have been utilized to prevent aggregation of nanoparticles during the application of plasma coating process. These include rotating reactors, fluidized bed reactors, mechanical mixing plasma reactors. Mechanical mixing within a fluidized bed is a good method to minimize aggregation and to test the feasibility of plasma coating/treatment of nanomaterials [13,14]. In this study, a magnetically assisted fluidized bed plasma reactor equipped with radio frequency (RF) plasma power supply was used for plasma nanocoating and treatment of MWCNTs [12,17]. The plasma conditions selected in this study were 100 mtorr of pressure, allylamine/argon mixture at 1:1 ratio, 6 watts of RF power input, 30 min of plasma treatment time for each batch treatment of 1.0 gram of MWCNTs. The resulted plasma nanocoated MWCNTs were characterized by surface contact angle measurement using water and resin respectively, Fourier transform infrared (FTIR) spectroscopy, aqueous pH change measurement, and high resolution TEM.

For surface contact angle measurement, untreated and plasma nanocoated MWCNTs samples were pressed into pellets between two polished 316 stainless steel plates using a Carver (Wabash, IN) press with 3,000 lbs of force for 0.1 g of MWCNTs. The sessile droplet method by placing 0.3  $\mu\text{L}$  of deionized water droplets or  $\sim 20$   $\mu\text{L}$  of resin droplets on the surface of the pellets was used to determine the surface contact angle of MWCNTs with a VCA 2500XE surface contact angle measurement system from Advanced Surface Technologies, Inc. (Billerica, MA, USA).

When 1.0 wt % MWCNTs was introduced to the viscous Epon 815C resin (Miller Stephenson), the filler was dispersed via a ultra-sonic horn (450 Sonifier, Branson, Danbury, CT) at a micro tip limit of 8 (power setting) with 50% duty cycle for 4 min. Curing agent, 12 wt % of Epicure 3223 was then added into the Epon 815C epoxy and well mixed. Immediately afterwards, a sample was poured into a dog bone shaped mold (ASTM D638-08). The dog bone mold was made by machining 1/8" aluminum sheet by a computer aided milling machine. Teflon release spray (Miller Stephenson) was applied to the mode surfaces prior to introducing the epoxy mixture. Then the mold was assembled and put in a 100 °C oven to cure for 1 h. Cross-section area of the dog bone shape test specimens ( $\sim 1/8'' \times 1/4''$ ) was measured by digital caliper prior to tensile testing. Tensile test of the dog bone shape specimens thus prepared was performed using a Series 812 Materials Test System, universal testing machine. The cross-sections of the tested specimens were characterized by TEM and optical imaging. The TEM images were obtained using a JEOL JEM-1400 transmission electron microscope operated at 140 kV accelerating voltage. The HRTEM images were acquired by a JEOL 2100 high resolution transmission electron microscope operated at 200 kV accelerating voltage. The fractured surfaces of the tested

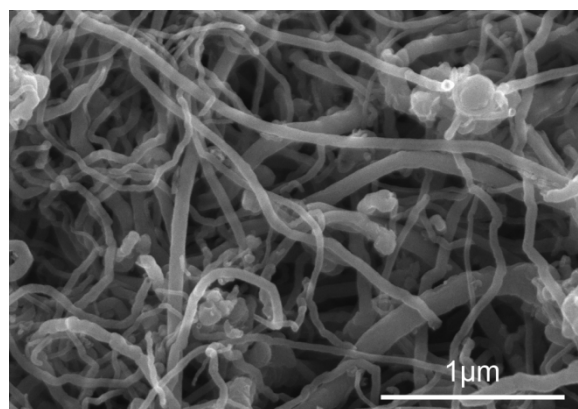
specimens were analyzed both visually and by SEM. For SEM measurements, 5 nm platinum coating was sputter coated on the fracture surfaces to reduce charging for imaging by SEM.

Powdered epoxy samples were produced with 600 grit SiC abrasive paper for differential scanning calorimetry (DSC) measurements (Pyris Diamond, Perkin-Elmer Corp., Norwalk, CT, USA). DSC measurements were performed from 30 to 150 °C with scanning rate of 5 °C per minute.

### 3. Results and Discussion

An SEM image of the MWCNTs used in this study is shown in Figure 2. The as-received MWCNTs tend to be tortuous. This indicates the MWCNTs have a large quantity of defects exist. Tortuous nanotubes are believed to affect the composite more as whiskers than 0.5 ~ 40 μm long tubes due to their relative low aspect ratio in a single direction. Wong and Sheehan experimentally determined bending strengths of MWCNTs to average around  $14.2 \pm 8.0$  GPa with diameters 26–76 nm (highest strength observed was 28.5 GPa) [23]. The quality of the MWCNTs could affect the strength [24]. The whisker-like MWCNTs can still significantly reinforce a polymer composite if the interface between the MWCNTs and the matrix provide a sufficient load transfer. A proper surface treatment of MWCNTs could provide an improved interface between the MWCNT and a polymer matrix.

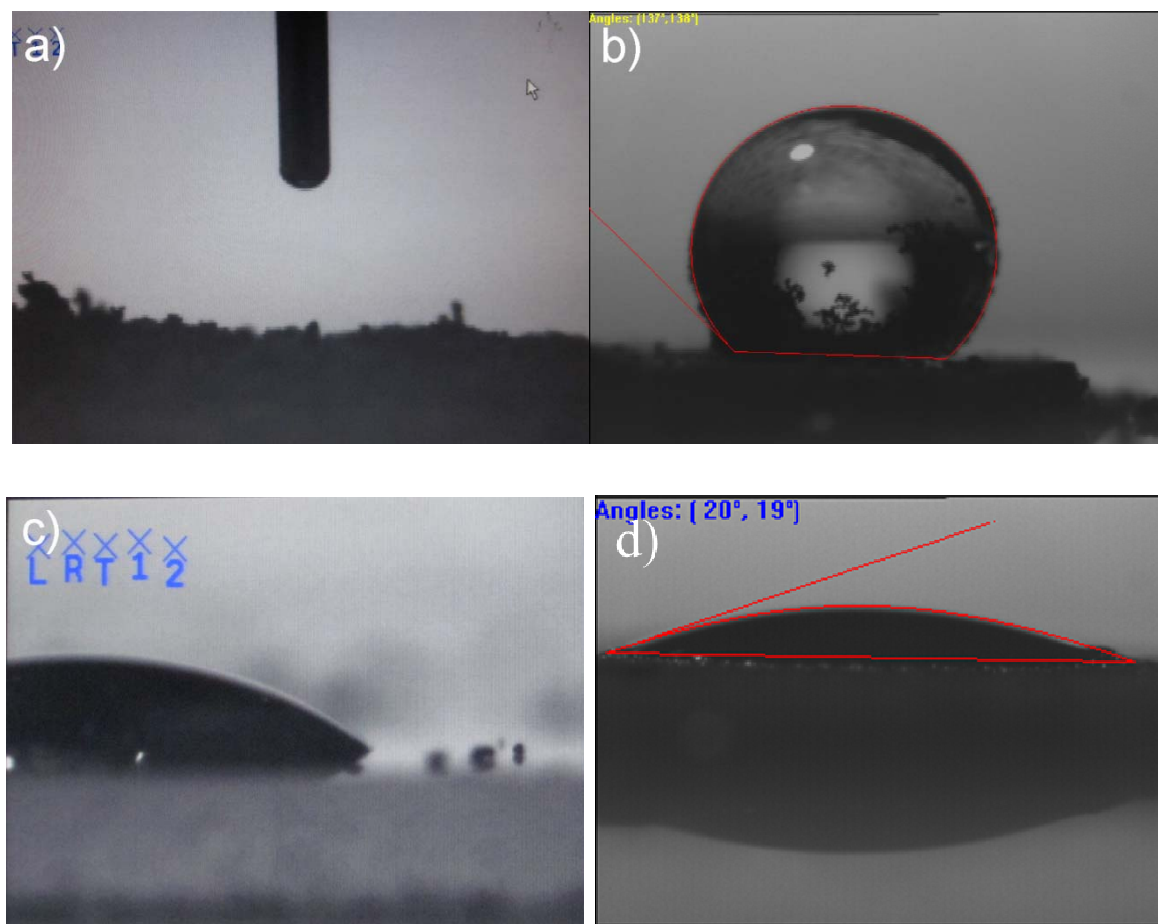
**Figure 2.** SEM image of the as-received MWCNTs with diameter of 60–100 nm.



After plasma treatment the MWCNTs mass was measured and the sample was separated into two groups, with one group for surface characterization and another for the MWCNT reinforced epoxy nanocomposite preparation. Contact angle measurement results showed the plasma nanocoating induced a significant change in surface energies of MWCNTs. Without plasma nanocoating, the pressed MWCNT pellet completely absorbed the water droplets placed on the pellet surface for contact angle measurements (Figure 3(a)). This phenomenon was probably due to oxidized defects existed on the MWCNT surface. Such oxidized defects are commonly found on carbon nanotube surfaces and would render the MWCNTs hydrophilic [9,25]. After the plasma coating MWCNTs became hydrophobic and had water contact angles averaging to 137° (Figure 3(b)). The plasma coating could provide a hydrophobic surface on the MWCNTs by encapsulating the MWCNTs and thus covering their hydrophilic oxidized defects. Surface contact angle measurements were also performed using Epon 815C resin in order to achieve a better understanding of the interactions of the MWCNTs with

the epoxy matrix. When Epon 815C resin droplets came into contact with the surface of the uncoated MWCNT pellets, the resin was slowly absorbed into the MWCNTs and it took about 10 ~ 15 s. Figure 3(c) shows the Epon 815C droplet image on the pressed pellet of untreated MWCNTs. In contrast, the pressed pellet of plasma coated MWCNTs quickly and completely absorbed the Epon 815C resin droplet in ~3 s, which was much faster than that on untreated MWCNTs. Figure 3(d) shows the Epon 815C resin droplet image that was taken within 1 s after it was placed on the pellet surface pressed from plasma coated MWCNTs. Penetration of the epoxy resin into the pressed pellet and quick spreading of the epoxy resin on the pellet surface were clearly observed from Figure 3(d).

**Figure 3.** Representative optical images of the sessile droplet measurement on pressed pellets of (a) 60–100 nm diameter MWCNTs with distilled water, (b) plasma nanocoated 60–100 nm diameter MWCNTs with distilled water, (c) 10–30 nm diameter MWCNTs with Epon 815C resin, and (d) plasma nanocoated 10–30 nm diameter MWCNTs with Epon 815C resin.



Dispersion tests did not show any visual difference between plasma nanocoated MWCNTs and the untreated controls in the Epon 815C resin after setting for 30 days. However after transferring the mixture from one vial to another vial, a noticeable quantity of uncoated MWCNT aggregation was observed at the vial bottom. In contrast, little to no aggregation was observed for plasma nanocoated samples. These results indicated that plasma nanocoated MWCNTs did provide better interaction with the epoxy matrix than the untreated MWCNT controls.

Figure 4 shows the high-resolution TEM images of untreated and plasma coated MWCNTs. It was found that a layer of 1 nm thick amorphous plasma nanocoating was observed on plasma nanocoated MWCNT surfaces, but not on the uncoated MWCNTs. The aqueous pH value measured with plasma nanocoated MWCNTs dispersed in water increased by 2.01 compared to only an increase of 0.24 for uncoated MWCNTs in water. This indicates that the surface amine functionalities on plasma nanocoated MWCNTs could be protonated when dispersed in water. These amine functionalities could covalently bond to the epoxy matrix and provide a strong interface. FTIR spectroscopic measurements of both untreated and plasma coated MWCNTs were performed. The resulted FTIR spectra contained large quantities of noise and did not provide much information about the plasma surface modification of MWCNTs. It was anticipated that the surface modification of MWCNTs by allylamine plasma nanocoating could enhance their dispersion in the epoxy, improve the filler/matrix interfacial interaction, and thus increase the mechanical properties of the resulted epoxy nanocomposite.

**Figure 4.** High resolution TEM images of (a) 10–30 nm diameter MWCNTs and (b) plasma nanocoated 10–30 nm diameter MWCNTs, in which the arrow points to the ~1 nm plasma nanocoating on the MWCNT surface.

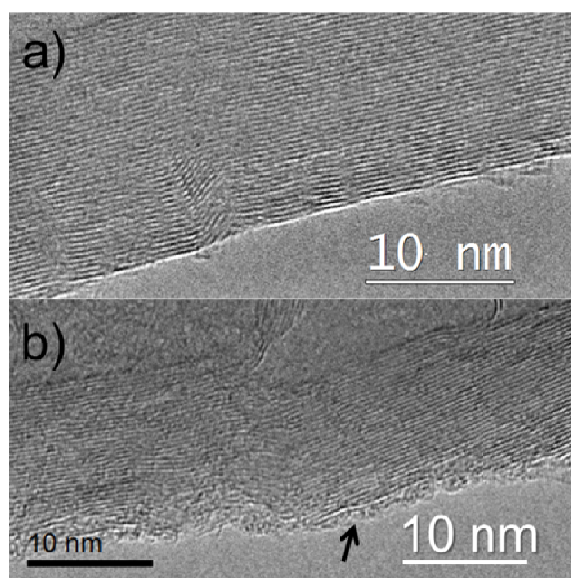


Table 1 shows the tensile test results of pure epoxy and the epoxy nanocomposites reinforced with untreated and plasma nanocoated MWCNTs. In comparison with the pure epoxy control, the epoxy nanocomposites prepared with untreated MWCNTs showed a decrease in ultimate tensile strength. In contrast, plasma nanocoated MWCNTs reinforced epoxy nanocomposites showed vast improvement compared to the pure epoxy. Epoxy nanocomposites reinforced by plasma nanocoated MWCNTs gave a tensile strength of 105.28 MPa, more than 50% increase from the pure epoxy controls. The measured Young's Modulus of pure epoxy control was 2.14 GPa; in contrast Young's Modulus of the plasma nanocoated MWCNT reinforced epoxy nanocomposite increased by 13.2%. The modulus of epoxy with addition of untreated MWCNTs also showed an increase in modulus. It is important to note that certain plasma nanocoated MWCNT reinforced epoxy nanocomposite test specimens failed at the clamp during testing, implying that the test section is stronger than the recorded values. It was noted

that plasma nanocoated MWCNT reinforced epoxy nanocomposite test specimens had the largest ultimate strain of 0.29, as compared with the value of 0.16 measured with the pure epoxy control specimens.

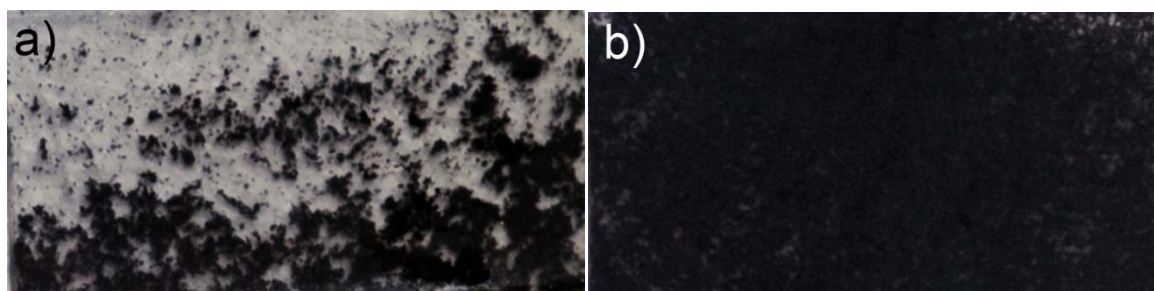
**Table 1.** Tensile test results of pure epoxy (Epon 81C), and its nanocomposites reinforced with 1.0 wt % untreated MWCNTs and plasma nanocoated MWCNTs.

Filler	Ultimate Strength (MPa)	Young's Modulus (GPa)	Ultimate Strain (%)
Pure Epoxy	68.46 ± 5.71	2.141 ± 0.090	0.16 ± 0.03
Epoxy/untreated MWCNT (60–100 nm indiameter)	45.40 ± 16.48	2.360 ± 0.137	0.11 ± 0.04
Epoxy/untreated MWCNT (10–30 nm in diameter)	62.30 ± 11.40	2.340 ± 0.254	0.13 ± 0.02
Epoxy/plasma nanocoated MWCNT (10–30 nm in diameter)	105.28 ± 32.58	2.424 ± 0.101	0.29 ± 0.18

The test results were expressed in mean ± standard deviation.

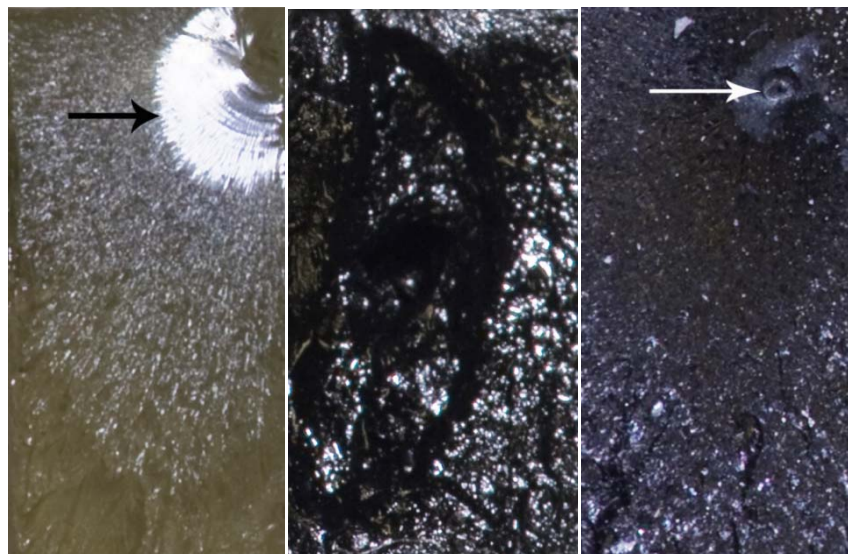
Digital photographs of the cross section of the epoxy nanocomposite specimens showed that untreated MWCNTs settled to the bottom of the cross-section of their composites as seen in Figure 5(a). In contrast the cross-section of the epoxy composites reinforced by plasma nanocoated MWCNTs had uniform dispersion of the MWCNTs through the epoxy nanocomposite specimen as shown in Figure 5(b). This result indicates that surface modification of MWCNTs using allylamine plasma nanocoating significantly improved the dispersion property of MWCNTs in epoxy matrices.

**Figure 5.** Digital photograph images of a cross-section of epoxy composite material reinforced with (a) untreated 10–30 nm diameter MWCNTs and (b) plasma nanocoated 10–30 nm diameter MWCNTs.



Fracture surfaces of the pure epoxy controls and the epoxy nanocomposite reinforced with unmodified MWCNTs varied significantly. As shown in Figure 6, a mirror zone, rib marks, and hackles could be visually seen on pure epoxy control samples, while composite samples reinforced with untreated MWCNTs revealed rough fracture surfaces and in many instances two uneven fracture surfaces. The uneven fracture surfaces could be another indication of uneven loading of MWCNTs within the composite. In contrast, epoxy nanocomposites reinforced by plasma nanocoated MWCNTs have a smaller mirror zone than pure epoxy control samples which indicate a high strength composite.

**Figure 6.** Digital photograph of fractured cross sections of pure epoxy (**right**), epoxy composite reinforced by untreated 10–30 nm diameter MWCNTs (**middle**), and epoxy composite reinforced by plasma treated 10–30 nm diameter MWCNTs (**left**). The arrows point to the mirror zone induced by fracture.



Fracture surfaces of epoxy nanocomposite reinforced with untreated MWCNTs were examined under high resolution HR SEM and no fiber pullout was found. In some samples aggregates of untreated MWCNTs were observed in the fracture surface, although these were rare occurrences. Figure 7 shows a representative SEM image with fiber pullout on the fracture surface of plasma nanocoated MWCNT reinforced epoxy nanocomposite samples. MWCNT loading in the epoxy was relatively small and gave infrequent pullout; however pullout was observed over most of the mirrored fracture surface. The average diameter of the plasma nanocoated MWCNTs found on the fracture surface was around 50 nm, much larger than the diameter of the original 10–30 nm MWCNTs. TEM images show the plasma nanocoating on the MWCNTs was less than 1 nm as seen in Figure 4 and the platinum coating was less than 5 nm. This result implies that the remaining 8 nm was due to the epoxy binding to the plasma nanocoated MWCNT surfaces. The strong bonding observed is believed to be from covalent bonding between the amines on the plasma nanocoated MWCNTs and the Epon 815C resin through interfacial interaction mechanism illustrated in Figure 1. The tortuous nature of MWCNTs is believed to be a factor in the length of the fiber pullout.

**Figure 7.** SEM images of fracture surface of epoxy composite reinforced by plasma nanocoated 10–30 nm diameter MWCNTs at (a) 10k $\times$  and (b) 80k $\times$  magnification.

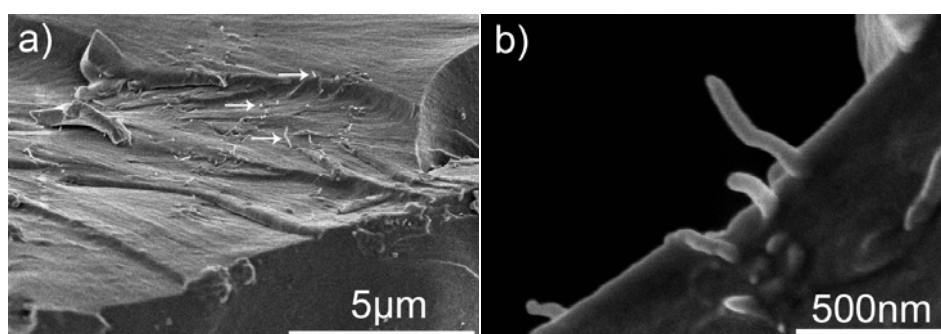
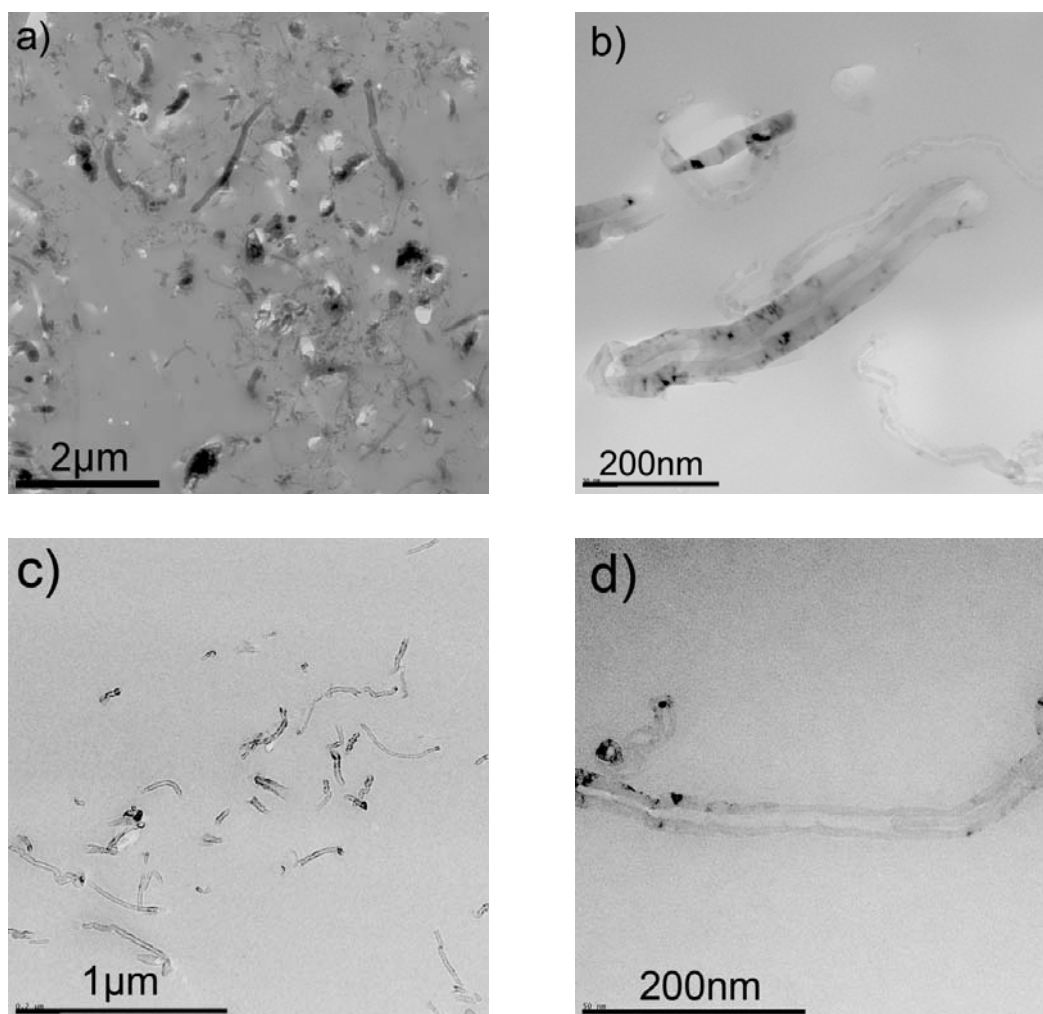


Figure 8 shows typical TEM images of the epoxy nanocomposite samples prepared with untreated and plasma nanocoated MWCNTs. It can be seen that, from Figure 8(a,b) for untreated MWCNT reinforced epoxy composite samples, areas of highly agglomerated MWCNTs was observed, where other locations had no MWCNTs. In contrast, when plasma nanocoated MWCNTs were used for epoxy nanocomposite fabrication with TEM images shown in Figure 8(c,d), both nano- and micro-scopic dispersion of plasma nanocoated MWCNTs in epoxy matrices was much uniform. It was also noticed that, the TEM images shown in Figure 8, almost all the MWCNT fillers observed in the nanocomposite samples had lengths less than 2  $\mu\text{m}$ , which is much shorter than the original MWCNT length. This observation could be due to the TEM sample preparation using microtome, which may cause pulling out and even fracture of longer MWCNTs. It might also due to the partially fracture of MWCNTs during their ultrasonic dispersion in epoxy resins. Sonication is known to fracture and shorten the length of reinforcing fibers and tubes [26,27].

**Figure 8.** TEM images of microtomed epoxy composite reinforced by (a,b) untreated 60–100 nm diameter MWCNTs, and (c,d) plasma nanocoated 10–30 nm diameter MWCNTs at various magnifications.



Digital and TEM images indicated poor dispersion of untreated MWCNTs in epoxy on both macro and micro scales. The reasons for the increased strength obtained for epoxy nanocomposite reinforced

with the plasma nanocoated MWCNTs are believed to be two-fold. First the surface modification of MWCNTs via plasma nanocoating allows their better dispersion throughout the epoxy resin. Second the plasma nanocoating provides surface amine functionalities, which provide chemical bonding formation between the plasma nanocoated MWCNT nanofillers and the epoxy resin during curing process and thus enhance the interfacial bonding between the filler and matrix for improved load transfer.

The contributions of interfacial bonding to composite strength can be estimated from micromechanics. There are several models that one can apply to calculate the strength of a composite reinforced with randomly oriented short fibers. Friend has proposed an equation of composite strength ( $\sigma_c$ ) based on the shear lag theory:  $\sigma_c = C\sigma_{fu}V_f(1 - L_c/2L) + (1 - V_f)\sigma_m^*$ , where  $C = 3/8$  or  $1/5$  for 2D or 3D random fiber distributions, respectively [28]. The term  $V_f$  is the fiber volume fraction,  $\sigma_{fu}$  is the tensile failure strength of the fiber,  $\sigma_m^*$  is the matrix strength at the fiber failure strain, and  $L$  is the fiber length. The term  $L_c$  is called the critical length or ineffective length, given by  $L_c/d = \sigma_{fu}/2\tau$ , in which  $d$  is the fiber diameter and  $\tau$ , is the interfacial shear strength. In the case of a strong interfacial bond,  $\tau$  is limited by the shear strength of the matrix. Assuming isotropy of the matrix this results in  $\tau = \sigma_m^*/\sqrt{3}$  [29] It has been shown that the interfacial friction derived from micromechanics is still valid for nanoscale interface [30]. Although the shear-lag model was not validated for describing the load transfer at nanotube/polymer interface, we assume that the above theory can be applied to nanotube/polymer composites. Taking the average values of  $d = 20$  nm,  $L = 10$   $\mu$ m,  $V_f = 0.01$ ,  $\sigma_m^* = 68.4$  MPa,  $\sigma_{fu} = 14.2 \pm 8$  GPa, then  $\sigma_c$  is in the range of 80.1 ~ 112.1 MPa, with an average strength of 96 MPa for strong interfacial bonding ( $L \ll L_c$ ). The predictions are in good agreement with the experimental results ( $\sigma_c = 105$  MPa) for plasma nanocoated MWCNTs epoxy composites. This result suggests that plasma coating significantly improves the interface and makes the MWCNTs fully functioning as reinforcement in polymer matrix composites.

**Table 2.** Thermal properties of MWCNT epoxy composites measured using differential scanning calorimetry (DSC).

Sample	$T_g$ ( $^{\circ}$ C)	$C$ ( $J/kg$ $^{\circ}$ C)
Pure Epoxy	68.37	2.403
Epoxy/untreated MWCNTs (10–30 nm in diameter)	69.36	1.854
Epoxy/plasma nanocoated MWCNTs (10–30 nm in diameter)	70.19	1.74

The thermal properties of the MWCNT reinforced nanocomposite also changed from pure epoxy. As seen from Table 2, the glass transition temperatures only varied a couple of degrees with 1% MWCNT addition in the epoxy composite. This is consistent with the common observation in carbon nanotube polymer composites [31,32]. The heat capacity on the other hand significantly decreased from 2.403  $J\ kg^{-1}\ ^{\circ}C^{-1}$  for pure epoxy to 1.854  $J\ kg^{-1}\ ^{\circ}C^{-1}$  for untreated MWCNT reinforced epoxy composite samples, and further down to 1.740  $J\ kg^{-1}\ ^{\circ}C^{-1}$  for plasma nanocoated MWCNT reinforced epoxy composite samples. This implies an enhanced interfacial interaction between MWCNTs and the

epoxy matrix, where plasma nanocoated MWNT further enhances this interaction [26,27]. The MWCNTs could also act as heat sinks distributing the heat through the composite with a higher efficiency than pure epoxy. The percolation threshold of the material should be much greater than 1% with tubes diameters of 10–30 nm. Increased plasma nanocoated MWCNT loading could further decrease the heat capacities as currently observed.

#### 4. Conclusion

Allylamine plasma nanocoated MWCNTs significantly increased the tensile strength of their epoxy nanocomposite by 54%, while the untreated MWCNTs decreased the tensile strength of the epoxy composite. Fractographical analysis of the epoxy composites containing untreated MWCNTs indicated a poor dispersion of MWCNT filler. SEM images of the fracture surface of epoxy composites containing plasma nanocoated MWCNTs showed fiber pullout, an important toughening mechanism in composites. The photograph of a thin cross section of the resulted composites containing untreated MWCNTs showed that the MWCNTs settled within the composite. Surface modification of MWCNTs by allylamine plasma nanocoatings significantly increased the dispersion of the nanofillers within the epoxy matrix as indicated by optical photography, optical microscopy, SEM analysis, and TEM analysis. Heat capacity decreased from  $2.403 \text{ J kg}^{-1} \text{ }^\circ\text{C}^{-1}$  for pure epoxy to  $1.740 \text{ J kg}^{-1} \text{ }^\circ\text{C}^{-1}$  for plasma nanocoated MWCNT reinforced epoxy composite samples, which indicated enhanced interfacial interactions between the nanofillers and polymer matrix. Simulation results based on the shear-lag model derived from micromechanics also confirmed that plasma nanocoating on MWCNTs significantly improved the epoxy/nanofillers interface bonding and as a result the increased composite strength. It was concluded that plasma nanocoating can be used to effectively modify nanofiller surfaces for fabrication of polymeric composite with significantly improved mechanical strength.

#### Acknowledgements

The authors would also like to thank the *US Department of Education (DOE) Graduate Assistance in Areas of National Need (GAANN) Fellowship* for the financial support to *Andy Charles Ritts*, who was a GAANN fellow.

#### References

1. Ajayan, P.M.; Tour, J.M. Materials science: Nanotube composites. *Nature* **2007**, *447*, 1066-1068.
2. Breuer, O.; Sundararaj, U. Big returns from small fibers: A Review of polymer/carbon nanotube composites. *Polym. Composite*. **2004**, *25*, 630-645.
3. Thostenson, E.T.; Li, C.; Chou, T.-W. Nanocomposites in context. *Composite. Sci. Technol.* **2005**, *65*, 491-516.
4. Thostenson, E.T.; Ren, Z.; Chou, T.-W. Advances in the science and technology of carbon nanotubes and their composites: A review. *Composite. Sci. Technol.* **2001**, *61*, 1899-1912.

5. Xia, Z.; Riester, L.; Curtin, W.A.; Li, H.; Sheldon, B.W.; Liang, J.; Chang, B.; Xu, J.M. Direct observation of toughening mechanisms in carbon nanotube ceramic matrix composites. *Acta Mater.* **2004**, *52*, 931-944.
6. Vaia, R.A.; Wagner, H.D. Framework for nanocomposites. *Mater. Today* **2004**, *7*, 32-37.
7. Wang, H.; Zeng, C.; Elkovitch, M.; Lee, L.J.; Koelling, K.W. Processing and properties of polymeric nano-composites. *Polym. Eng. Sci.* **2001**, *41*, 2036-2046.
8. Hussain, F.; Hojjati, M.; Okamoto, M.; Gorga, R.E. Review article: Polymer-matrix nanocomposites, processing, manufacturing, and application: An overview. *J. Composite Mater.* **2006**, *40*, 1511-1575.
9. Bahr, J.L.; Tour, J.M. Covalent chemistry of single-walled carbon nanotubes. *J. Mater. Chem.* **2002**, *12*, 1952-1958.
10. Chen, Q.; Dai, L.; Gao, M.; Huang, S.; Mau, A. Plasma activation of carbon nanotubes for chemical modification. *J. Phys. Chem. B* **2001**, *105*, 618-622.
11. Gao, Y.; He, P.; Lian, J.; Wang, L.; Qian, D.; Zhao, J.; Wang, W.; Schulz, M.J.; Zhang, J.; Zhou, X.; Shi, D. Improving the mechanical properties of polycarbonate nanocomposites with plasma-modified carbon nanofibers. *J. Macromol. Sci. Part B* **2006**, *45*, 671-679.
12. Guo, Y.; Cho, H.; Shi, D.; Lian, J.; Song, Y.; Abot, J.; Poudel, B.; Ren, Z.; Wang, L.; Ewing, R.C. Effects of plasma surface modification on interfacial behaviors and mechanical properties of carbon nanotube-Al<sub>2</sub>O<sub>3</sub> nanocomposites. *Appl. Phys. Lett.* **2007**, *91*, 261903.
13. Shi, D.; Lian, J.; He, P.; Wang, L.M.; Ooij, W.J.V.; Schulz, M.; Liu, Y.; Mast, D.B. Plasma deposition of ultrathin polymer films on carbon nanotubes. *Appl. Phys. Lett.* **2002**, *81*, 5216-5218.
14. Shi, D.; Lian, J.; He, P.; Wang, L.M.; Xiao, F.; Yang, L.; Schulz, M.J.; Mast, D.B. Plasma coating of carbon nanofibers for enhanced dispersion and interfacial bonding in polymer composites. *Appl. Phys. Lett.* **2003**, *83*, 5301-5303.
15. Shi, D.; Wang, S.X.; Ooij, W.J.V.; Wang, L.M.; Zhao, J.; Yu, Z. Uniform deposition of ultrathin polymer films on the surfaces of Al<sub>2</sub>O<sub>3</sub> nanoparticles by a plasma treatment. *Appl. Phys. Lett.* **2001**, *78*, 1243-1245.
16. Shi, D.; He, P.; Lian, J.; Wang, L.; Ooij, W.J.V. Plasma deposition and characterization of acrylic acid thin film on ZnO Nanoparticles. *J. Mater. Res.* **2002**, *17*, 2555-2560.
17. Yu, Q.; Kim, Y.J.; Ma, H. Plasma treatment of diamond nanoparticles for dispersion improvement in water. *Appl. Phys. Lett.* **2006**, *88*, 231503.
18. Ávila-Orta, C.A.; Cruz-Delgado, V.J.; Neira-Velázquez, M.G.; Hernández-Hernández, E.; Méndez-Padilla, M.G.; Medellín-Rodríguez, F.J. Surface modification of carbon nanotubes with ethylene glycol plasma. *Carbon* **2009**, *47*, 1916-1921.
19. Naseh, M.V.; Khodadadi, A.A.; Mortazavi, Y.; Pourfayaz, F.; Alizadeh, O.; Maghrebi, M. Fast and clean functionalization of carbon nanotubes by dielectric barrier discharge plasma in air compared to acid treatment. *Carbon* **2010**, *48*, 1369-1379.
20. Ren, X.; Shao, D.; Zhao, G.; Sheng, G.; Hu, J.; Yang, S.; Wang, X. Plasma induced multiwalled carbon nanotube grafted with 2-vinylpyridine for preconcentration of Pb(II) from aqueous solutions. *Plasma Process. Polym.* **2011**, *8*, 589-598.

21. Xu, L.; Fang, Z.; Song, P.A.; Peng, M. Functionalization of carbon nanotubes by corona-discharge induced graft polymerization for the reinforcement of epoxy nanocomposites. *Plasma Process. Polym.* **2010**, *7*, 785-793.
22. Xu, L.; Fang, Z.; Song, P.A.; Peng, M. Surface-initiated graft polymerization on multiwalled carbon nanotubes pretreated by corona discharge at atmospheric pressure. *Nanoscale* **2010**, *2*, 389-393.
23. Wong, E.W.; Sheehan, P.E. Nanobeam mechanics: Elasticity, strength, and toughness of nanorods and nanotubes. *Science* **1997**, *277*, 1971-1975.
24. Qian, D.; Dickey, E.C.; Andrews, R.; Rantell, T. Load transfer and deformation mechanisms in carbon nanotube-polystyrene composites. *Appl. Phys. Lett.* **2000**, *76*, 2868-2870.
25. Burch, H.J.; Contera, S.A.; De Planque, M.R.R.; Grobert, N.; Ryan, J.F. Doping of carbon nanotubes with nitrogen improves protein coverage whilst retaining correct conformation. *Nanotechnology* **2008**, *19*, 384001.
26. He, P.; Gao, Y.; Lian, J.; Wang, L.; Qian, D.; Zhao, J.; Wang, W.; Schulz, M.J.; Zhou X.P.; Shi, D. Surface modification and ultrasonication effect on the mechanical properties of carbon nanofiber/polycarbonate composites. *Composite. Part A: Appl. Sci. Manuf.* **2006**, *37*, 1270-1275.
27. Baddour, C.E.; Briens, C.L.; Bordere, S.; Anglerot, D.; Gaillard, P. An investigation of carbon nanotube jet grinding. *Chem. Eng. Process.: Process Intensification* **2008**, *47*, 2195-2202.
28. Friend, C.M. The effect of matrix properties on reinforcement in short alumina fibre-aluminium metal matrix composites. *J. Mater. Sci.* **1987**, *22*, 3005-3010.
29. Van Hattum, F.W.J.; Bernardo, C.A. A model to predict the strength of short fiber composites. *Polym. Composite.* **1999**, *20*, 524-533.
30. Li, L.; Xia, Z.H.; Curtin W.A.; Yang, Y.Q. Molecular dynamics simulations of interfacial sliding in carbon-nanotube/diamond nanocomposites. *J. Amer. Ceram. Soc.* **2009**, *92*, 2331-2336.
31. Shieh, Y.-T.; Liu, G.-L. Effects of carbon nanotubes on crystallization and melting behavior of poly(L-lactide) via DSC and TMDSC studies. *J. Polym. Sci. Part B: Polym. Phys.* **2007**, *45*, 1870-1881.
32. Xia, H.; Song, M. Preparation and characterisation of polyurethane grafted single-walled carbon nanotubes and derived polyurethane nanocomposites. *J. Mater. Chem.* **2006**, *16*, 1843-1851.